EXPERIMENTAL INVESTIGATION OF FLOW OBSTACLES EFFECT ON SINGLE PHASE HEAT TRANSFER

A. Tanase[*], D.C. Groeneveld[†*], H. Zahlan[*] and S.C. Cheng [*]

[*]University of Ottawa, Ottawa, ON Canada K1N 6N5
[†]Atomic Energy of Canada Limited, Chalk River, ON Canada K0J 1J0

Abstract

Previous experimental studies of the effect of flow obstacles on heat transfer in bundles suggest an analogy between the increased pressure drop at the flow obstacle, and the enhancement in wall heat transfer. Right behind the blockage, the flow decelerates and turbulent wakes are generated. The wakes agitate the wall boundary layer and enhance the heat transfer from the wall.

It was generally assumed that that heat flux, mass flux and shape of the flow obstruction do not play a major role on the heat transfer enhancement. To investigate these effects, an experiment was performed at the University of Ottawa's Thermalhydraulics Laboratory. The test section consisted of a directly heated Inconel 600 tube having inside diameter of 5.46 mm and the outside diameter of 8.00 mm, cooled internally by Freon 134a. The outside temperature of the test section was measured by six K type thermocouples, located in pairs, 180 deg apart at three planes. A flow obstacle, having a 24% obstruction ratio, was located inside the test section. A strong ceramic magnet, located on the outside of the test section, fixed the location of the obstacle, and allowed the relocation of the obstacle circumferentially and axially during the experiments. The heat transfer enhancement effect downstream of the obstacles was measured at 3 , 5, 7, 10, 20, 30, 50 and 70 diameters downstream the flow obstacle. Two obstacle leading and trailing edge shapes (streamlined and blunt, having the same obstruction ratio, 24%), four mass fluxes and six heat fluxes were investigated.

1. Introduction

Several experimental studies of the flow obstacle effect on heat transfer have been performed on bundle geometries. References [1-5], [9], [10], [13] discuss the analogy between the increased pressure drop at the flow obstacle such as a grid spacer, and the enhancement in wall heat transfer. Just downstream of the obstacle, the flow decelerates and turbulent wakes are generated. The wakes agitate the wall boundary layer and enhance the heat transfer from the wall. For simplicity, [13] assumed that the wake induced heat transfer augmentation is directly proportional to the obstacle pressure drop. Assuming that this assumption is valid, the equation for heat transfer augmentation due to the flow obstacles will be of a similar form as that for the pressure drop increase caused by the obstacle. This increase in heat transfer can be explained by a gradual contraction of the flow upstream of the obstacle. Using Equation 1, [9] correlated the maximum heat transfer augmentation at the obstacles on smooth rods in single-phase flow as

$$Nu/Nu_0 = 1+5.55\ \varepsilon^2 \qquad \text{Eqn. 1}$$

Where ε is the flow blockage ratio and Nu_0 is the Nusselt number for a channel without any flow obstacles. The Nusselt numbers reach a maximum at, or slightly downstream of the flow obstacle. Further downstream the hydrodynamic and thermal boundary layers are slowly approaching their fully developed profiles. This developing boundary layer phenomenon is similar to the entry length effect in turbulent tube flow. The augmentation of heat transfer has been observed to be an exponentially decaying function of z/D where z is the distance downstream of the obstacle.

$$Nu^* = Nu/Nu0 = 1+5.55\ \varepsilon^2\ exp(-0.13\ z/D) \qquad \text{Eqn. 2}$$

for Reynolds number higher than 10^4. Equation 2 shows a typical variation in heat transfer enhancement downstream of a bundle spacer for various flow blockage ratios. The results of [13] clearly show that there is an influence of the Reynolds number on the maximum and on the axial distribution of the Nusselt numbers for different blockage factors. The improvement in heat transfer due to the obstacle decreases with increasing Reynolds numbers for Re > 3000. For the same Reynolds number, the improvement in heat transfer is higher for higher flow blockage ratios. The reason is that higher flow blockage ratios produce higher flow velocities and turbulence resulting in a greater improvements in heat transfer [3]. The correlation proposed by [13] - Equation 2 - is applicable for a specific type of grids and does not take into account the obstacle-location effect on heat transfer enhancement

More recently, the authors of [8] have investigated the impact of various flow obstacles on single phase heat transfer, film boiling heat transfer and pressure drop based on internally cooled tube data. This paper describes the film boiling experiment with an obstacle-equipped tube and presents a new method for predicting the enhancement in heat transfer (expressed as Nu/Nu_0) for both the single-phase gas-cooled region and the post-dryout heat transfer region.

2. Experimental setup

The experiment was conducted in the multi-fluid test loop at University of Ottawa (Figure 1) using HFC-134a as working fluid. The main components of the loop are test section, condenser, pressurizer, pumps, preheaters, power supply and related instruments.

The test section is directly heated by a 12 kW DC power supply (40V, 300 A). The inlet and outlet fluid temperatures of the test section are measured by two RTDs. The flow is recirculated by two gear pumps, installed in series, and delivering a constant volumetric flow rate.

A bypass around the pumps controls the flow rate. The flow is measured by a Coriollis flow meter with an accuracy of better than 0.5% (flow range 0 – 0.34 kg s^{-1}). The pressure in the loop is controlled by the pressurizer. The pressurizer contains a heating coil, located at the bottom of the pressurizer, and a cooling coil near the top of the pressurizer. The power to the pressurizer heater (maximum 500 W) is regulated by an adjustable AC transformer. An electric pre-heater (maximum power 5 kW) and a coaxial heat exchanger (with hot water on the secondary side) are located between the pumps and the test section. They are used to adjust the test section inlet fluid temperature or inlet mass quality to the desired values. The vapour generated in the test section is condensed by a coaxial heat exchanger prior to the fluid being recirculated to the pump.

The experiment was performed in a DC heated Inconel 600 tube having an inside diameter of 5.46 mm, the outside diameter of 8.00 mm, and a heated length is Lh = 2 m. The experimental loop consists of two gear pumps, connected in series, two preheaters, mass flow measuring device, test section (see Figure 1), condenser (for two-phase flow experiments), pressurizer, filter and the recirculation valves. RTDs measure the bulk fluid temperature at the inlet and outlet of the test section(TS), a piezoelectric pressure sensor measures the absolute pressure at the outlet of TS, and a differential pressure sensor measures the ΔP along the TS.

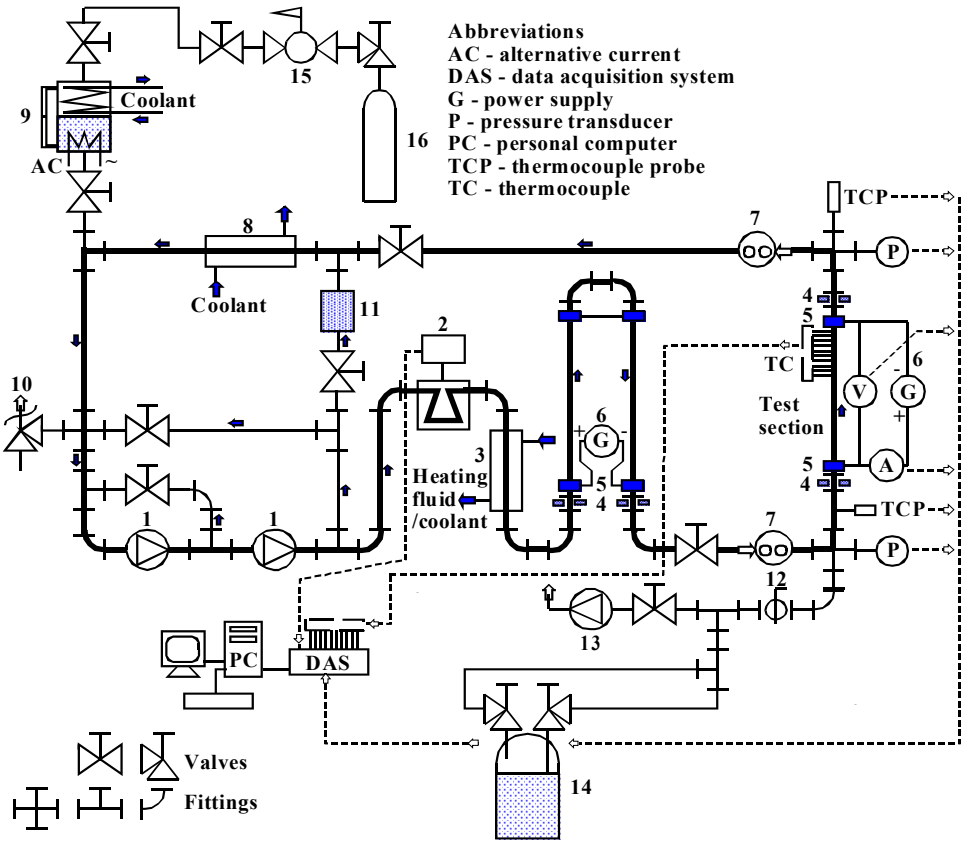

1-gear pump, 2-Coriollis type mass-flow-meter, 3-pre-heater, 4-dielectric fittings, 5-power terminals, 6-electrical pre-heater, 7-sight glass, 8-condenser, 9-pressurizer, 10-pressure relief valve, 11-refrigerant filter-dryer, 12-ball-valve, 13-vacuum pump, 14-refrigerant storage tank, 15-pressure reducer, 16-nitrogen container.

Figure 1 Experimental Multi-Fluid Loop (Vertical Test Section).

The outside temperature of the test section was measured by six K-type self-adhesive thermocouples (TC), located in pairs 180º apart at three planes (blue triangles in Figure 2). A flow obstacle, having a 24% obstruction ratio, was located inside the test section. A strong ceramic magnet, located on the outside of the test section, fixed the location of the obstacle. The obstacles have cylindrical shape, a length of 10 mm and a diameter 2.72 mm; they are manufactured from mild steel and located eccentrically in the test section (see Figure 2).

The L/D effect was measured at 3, 5, 7, 10, 20, 30, 50 and 70 diameters downstream from the flow obstacles. Two obstacle shapes (streamlined and blunt), four mass fluxes and six heat fluxes were investigated. The test matrix is shown in Table 1:

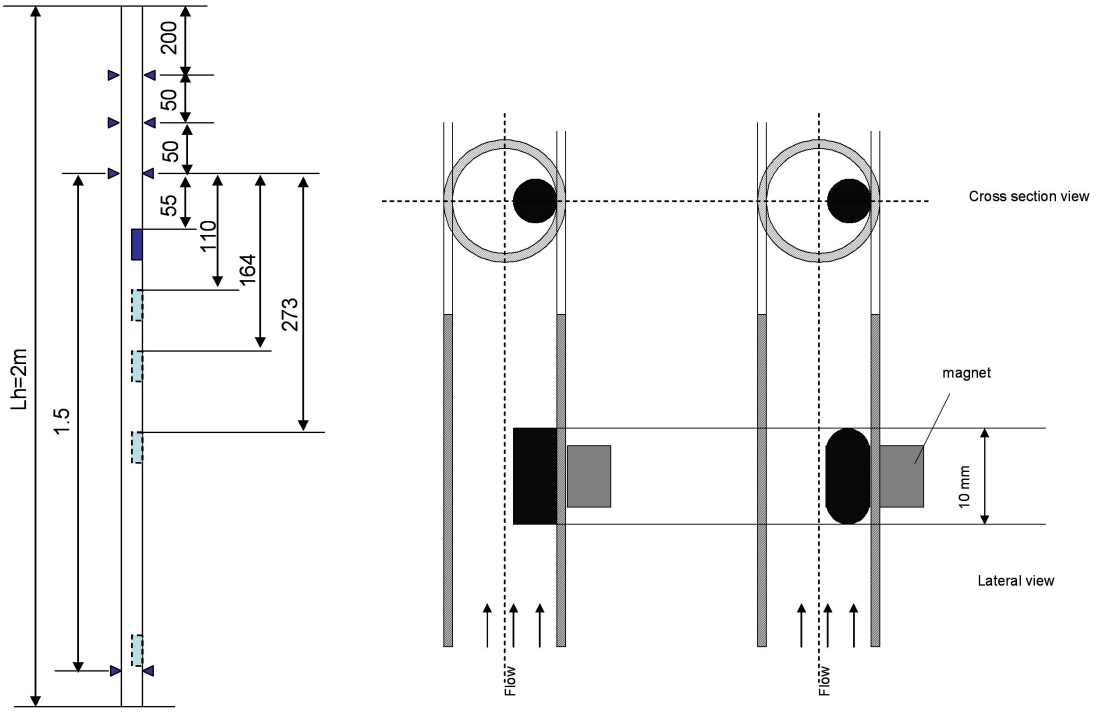

Figure 2: The schematic of test section, thermocouples and the obstacle layout

Table 1: Test matrix

G (kg m^{-2} s^{-1})	500			1000			2000			3500		
q_s (kW m^{-2})	10	15	20	15	20	35	20	35	60	35	60	120

The inlet fluid temperature for all experiments was 20 ºC. The experimental procedure followed these steps:

1. Set the inlet temperature at 20 ºC
2. Set the required mass flux
3. Place the obstacle far upstream from the TC locations (more than 100 L/D), in order to obtain the bare tube geometry. It is assumed that, for L/D > 100, no axial effect of obstacle on heat transfer is observed.
4. Set the required heat flux and wait for the system to reach steady conditions. If needed, the mass flux is readjusted.
5. Scan and record the reference (bare tube) data (take 10-15 scans, to be screened and averaged during the subsequent data processing)
6. While keeping the heat flux and mass flux steady, move the obstacle to 70 L/D upstream from the TC line. Scan and save.
7. Repeat (6) for all L/D considered in the test matrix.

2.1 Calibration and verification

Every three months the RTDs and thermocouples were re-calibrated using a single phase flow without heating the test section, two–phase inlet without heating the test section and at the onset of nucleate boiling method. The calibration tests confirmed an accuracy of 0.25 ºC for an interval between 20 and 80 ºC. In order to confirm the results, some tests were repeated randomly.

3. Results and discussion

The experimental results for two types of obstacles (round and blunt) having the same obstruction ratio, 24% are presented in Figure 3.

3.1 Effect of obstacle shape.

The obstacle shape has a significant influence at relatively short distances downstream obstacle (~ 3L/D). At low mass flux (500 kg $m^{-2}s^{-1}$) the blunt obstacle gives higher relative enhancement (42-50% for blunt shape compared to 32-38% for rounded) for the heat flux range investigated. The difference decreases as the mass flux increases and at G=1000 kg $m^{-2}s^{-1}$ although the blunt obstacle enhancement is still higher, the difference is less significant. At higher mass flux (approx 2000 kg $m^{-2}s^{-1}$) the round-shape obstacle seems to have noticeable higher relative enhancement that increases as the mass flux increases.

3.2 Effect of mass flux.

As mentioned by previous work, the relative heat transfer coefficient enhancement is dependent on Reynolds number of flow and, therefore, on the mass flux. For both types of obstacle and for all heat fluxes investigated the relative heat transfer coefficient enhancement decreases with increasing the mass flux, which confirm the previous findings. A novel finding from this research is that the variation of heat transfer enhancement with flow for blunt-type obstacles (from about 50% to 17%) is much larger than for rounded obstacles (from 35% to 27%).

3.3 Effect of heat flux.

It appears that the effect of heat flux is not significant, mixed trends have been noted but no clear effect can be found.

3.4 Effect of relative distance.

It has been reported previously ([1], [4], [10]) that the relative enhancement decays exponentially downstream from an obstacle. This is also confirmed by the observed trends of Figure 3, where it is shown that the enhancement becomes negligible at about L/D > 50 regardless of mass flux, heat flux or obstacle shape. An "unusual" trend occurs at L/D ~ 5 for the blunt shape obstacle (and to a smaller extent also for the rounded obstacle) at high mass flux, when a sudden decrease of relative enhancement is observed just downstream the obstacle. Although this effect is not specifically documented in the literature, it can be assumed that it is caused by the structure of the flow in the wake of a blunt obstacle. The investigators agreed that at the obstacle location the mechanism of convective heat flux enhancement is due to flow acceleration due to cross section reduction. At several relative distances downstream the flow deceleration occurs but the turbulence induced by the obstacle mixes the bulk fluid and the boundary layer, enhancing heat transfer. At high velocities flow separation at the trailing edge of the obstacle could have occurred and it appears that at several relative distances downstream obstacle the flow deceleration and/or flow reversal due to low pressure wake or large eddies which adversely affects the local heat transfer enhancement. For the current experiment the above mentioned effect becomes first noticeable at G = 2000 kg $m^{-2}s^{-1}$ and is much stronger for the blunt obstacle. Figure 3 shows that G=2000 kg $m^{-2}s^{-1}$ the maximum relative increase is at L/D = 3 but at L/D = 5-7 there is a local minimum followed by another local maximum at L/D = 10. This suggests that the wake region lasts for about 10 L/D, after which the diverted streamlines reattach to the heated wall and enhances the heat transfer coefficient (second

relative maximum). At G = 3500 kg $m^{-2}s^{-1}$ the maximum heat transfer enhancement is at L/D = 5 for the rounded obstacle and at L/D = 10 for the blunt one. These effects will be investigated further by subsequent measurements, CFD simulations and/or flow visualization (see Figure 4).

3.5 Comparison with the available prediction methods.

A direct comparison with Rehme's (1977) equation for heat transfer enhancement (Eqn.2) has been performed and suggests that this correlation underpredicts the relative enhancement in most cases (see Figure 3). The underprediction is greatest at low mass fluxes and becomes smaller as the mass flux increases. These results were somehow expected because the experiment suggests that the mass flux and the obstacle shape play also a significant role in the relative heat transfer enhancement, while Rehme's equation ignores these effects. Moreover, Rehme's equation can not predict the "unusual" trends found in the wake of an obstacle at high mass fluxes; therefore a more accurate prediction method is desirable.

3.6 Pressure loss coefficient (K) and relative heat transfer enhancement.

A supplementary investigation has been conducted in order to estimate the pressure loss coefficient for different types of obstacles (12% and 24% obstruction ratio, blunt and rounded flow obstacles). The experiments have been performed in adiabatic (zero heat flux) single phase flow and revealed a weak dependence of K in respect to Re: as Re increases, K decreases slightly (see Figure 5 a). From the same investigation it was found that the difference between the pressure loss coefficient for blunt and rounded obstacles is very high for the whole range of mass flux considered (1400 – 3500 kg $m^{-2}s^{-1}$). Although a significant difference in pressure loss coefficient between blunt and rounded obstacles was noticed, the difference in enhancement of heat transfer coefficient is minor. Moreover, it appears that at high flows, although the difference in K is high, at L/D>10 the relative enhancement is very close for both types of obstacles and at L/D<10 the rounded obstacle gives even better heat transfer augmentation (see Figure 5 b). It can be concluded that unlike two-phase flow, where the critical heat flux enhancement is strongly influenced by the obstacle shape, for the single phase the difference is minor, especially at L/D>10. Also, the hypothesis of proportionality between the pressure drop and the heat transfer enhancement, although intuitive and convenient may be questionable, at least for some geometries/flow conditions. As previously mentioned, the enhancement mechanisms downstream of an obstacle are very complex and new experiments and analysis should be performed to improve our understanding and to confirm the current findings.

4. Conclusion.

The present study is focused on the effect of obstacle shape, mass flux, heat flux and relative distance on the enhancement of heat transfer coefficient in a round tube. As reported in previous papers, flow obstacles significantly enhance the downstream heat transfer, the strongest effect being near the obstacle location. The heat transfer enhancement decays exponentially with distance downstream of the flow obstacle. A novel finding is that the enhancement decreases with an increase in mass flux for a constant L/D. The present experiment shows that the enhancement effect can be found up to 50 L/D, for various mass fluxes, obstacle shapes and heat fluxes. Unlike the blunt obstacle, the rounded obstacle shows relatively constant heat transfer enhancement over a large range of mass fluxes. The heat flux has a weak effect on relative heat transfer enhancement. The available prediction methods tend to underpredict the current experimental data.

5. References

1. Groeneveld, D.C., Yousef, W.W., Spacing devices for nuclear fuel bundles: a survey of their effect on CHF, post-dryout heat transfer and pressure drop. In: Proceedings of the ANS/ASME/NRC International Topical Meeting on Nuclear Reactor Thermal-Hydraulics, vol. 2, Saratoga Springs, New York, NY, October 5–8, pp. 1111– 1125. 719, 1980

2. Guo, Y., Groeneveld, D.C. and Cheng, S.C., Prediction of CHF enhancement due to flow obstacles, *Int. J. Heat Mass Transfer,* Vol 44, pp. 4557-4661*,* 2000

3. Hassan, M.A., Rehme, K., Heat transfer near spacer grids in gas-cooled rod bundles. Nucl. Technol. 52, 410– 414. 721, 1981

4. Hudina, M., Nothigen, H., Experiment Study of Local Heat Transfer under and near Grid Spacers Developed for GCFR, Swiss Federal Institute for Reactor Research Wirenlingen. Report TM-IN-526, 1972

5. Kidd, G.J., Hoffman, H.W., The Temperature Structure and Heat Transfer Characteristics of an Electrically Heated Model of a Seven-Rod Cluster Fuel Element, ASME 68-WA/HT-33, 1968.

6. Krett, V., Majer, J.,Temperature Field Measurement in the Region of Spacing Elements. Skoda Works
Nuclear Power Construction Department, Information Centre Plzen, Czechoslovakia. Report ZJE-114. 1971

7. Oka, Y., S. Koshizuka, T. Jevremovic and Y. Okano, Supercritical-pressure, light-water-cooled reactors for mproving economy, safety, plutonium utilization and environment", Prog. Nucl. Energy, Vol. 29 (supplement), pp. 31-438, 1995.

8. Pioro, I.L., Groeneveld, D.C., Cheng, S.C., Doerffer, S., Vasic, A.Z., Effect of flow obstruction shape on the critical heat flux. In: Proceedings of ICONE-8, Baltimore, MD, April 2–6, (paper #8350),2000

9. Rehme, K., Pressure drop of spacer grids in smooth and roughened rod bundles. Nucl. Tech. 31, 314–317, 1977

10. Stosic, Z., On the role of spacer grids on conditions of dryout/rewetting and local thermal hydraulics in boiling water channels, NURETH-9, San Francisco, California, Oct. 3 – 8, 1999

11. Tsiklauri, G., R. Talbert, B. Schmitt, G. Filippov, R. Bogoyavlensky and E. Grishanin, "Supercritical steam cycle for nuclear power plant", Nucl. Eng. Des., Vol. 235, pp. 1651-1664, 2005.

12. Vleck, J., Weber, P.,. The Experimental Investigation of A Local (Spot) Heat Transfer Coefficient in The Fuel Spacer Area. Australian Atomic Energy Commission Research Establishment Report LIB/TRANS 250, 1970

13. Yao, S.C., Hochreiter, L.E., Leech, W.J., Heat transfer augmentation in rod bundles near grid spacers. Heat Transfer 104 (1), 76–81. 778, 1982

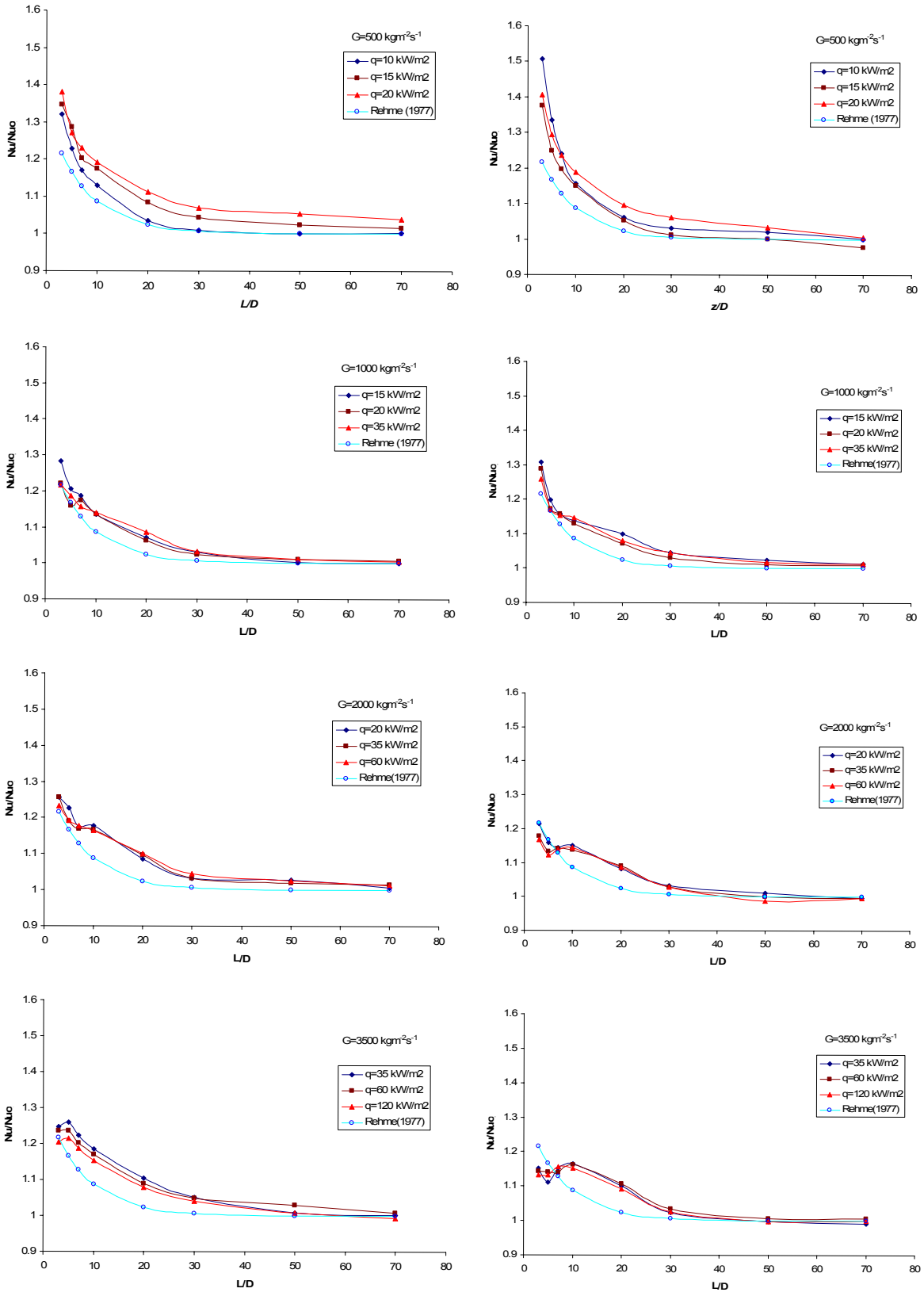

Figure 3 Nu/Nu_0 (enhanced/bare) versus relative distance (L/D) for various mass flux and heat flux, round shape obstacle (left) and blunt shape obstacle (right), 24% obstruction ratio.

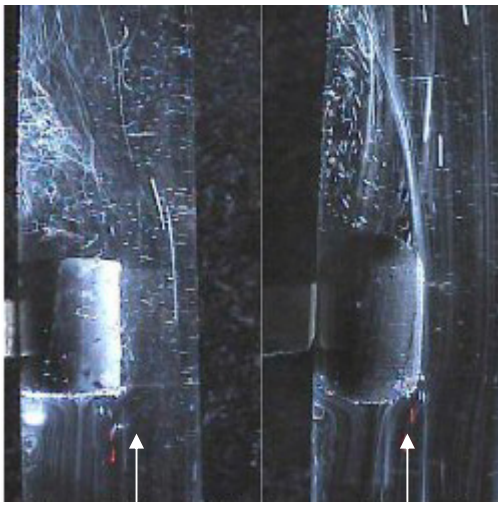

Figure 4 Flow visualization around blunt and rounded obstacle, Re~ 3000, upward flow direction

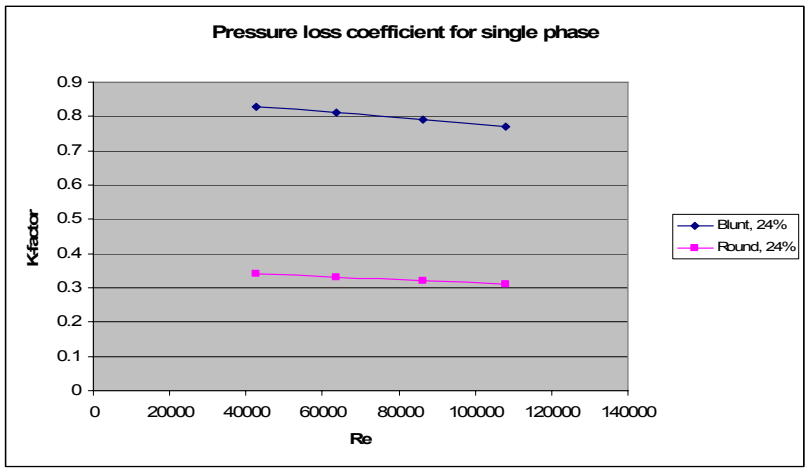

a)

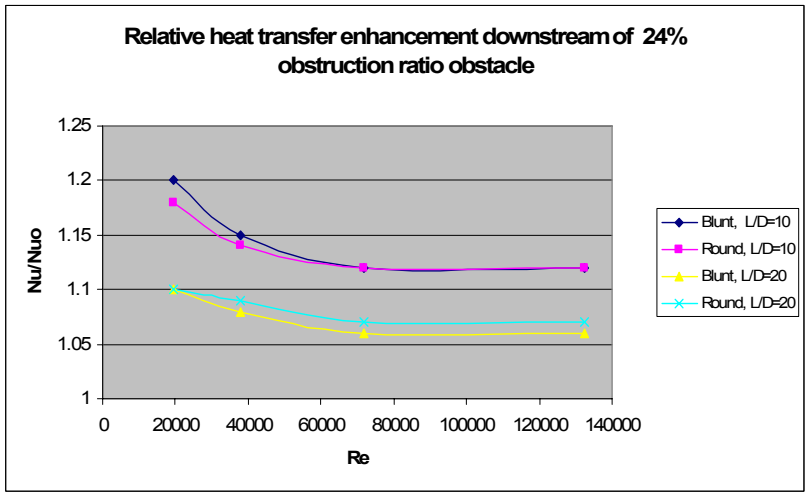

b)

Figure 5 Variation of pressure loss coefficient and the relative heat transfer enhancement in respect to Reynolds number